

Vanishing neoclassical viscosity and physics of the shear layer in stellarators

J. L. Velasco, J. A. Alonso, I. Calvo, and J. Arévalo

*Laboratorio Nacional de Fusión, Asociación EURATOM-CIEMAT, 28040 Madrid, Spain**

(Dated: August 11, 2021)

The drift kinetic equation is solved for low density TJ-II plasmas employing slowly varying, time-dependent profiles. This allows to simulate density ramp-up experiments and describe from first principles the formation and physics of the radial electric field shear layer. The main features of the transition are perfectly captured by the calculation, and good quantitative agreement is also found. The results presented here, that should be valid for other non-quasisymmetric stellarators, provide a fundamental explanation for a wealth of experimental observations connected to the shear layer emergence in TJ-II. The key quantity is the neoclassical viscosity, which is shown to go smoothly to zero when the critical density is approached from below. This makes it possible for turbulence-related phenomena, and particularly zonal flows, to arise in the neighborhood of the transition.

Understanding transport barriers in magnetic confinement devices [1] is a crucial issue for the fusion programme because they allow access to regimes of improved confinement in which commercial fusion reactors may be viable. Confinement transitions have been observed and comprehensively documented in a large variety of tokamaks and stellarators (see Ref. [2] and references therein). While the reduction of turbulence by sheared flows is generally accepted as a key ingredient in the transitions [3], the identification of the physical mechanisms that create these sheared flows is still an open issue. Zonal flows (i.e. turbulence-generated, fluctuating and flux-surface collective radial electric fields) are considered a possible catalyst of the transition, since they are observed close before confinement transitions and they are able to regulate transport [4]. In non-quasisymmetric stellarators, the non-ambipolar radial fluxes, and consequently the radial electric field, are basically determined by the neoclassical theory of collisional transport in magnetized plasma [5]. Therefore, the interaction between neoclassical and turbulent processes, and concretely the extent to which turbulence can overcome the neoclassical viscosity and modify the $E \times B$ rotation through momentum transport, has been the subject of recent works [4–7]. In this Letter, we contribute to the above programme with the study of the so-called low density confinement transition [8–12] in the flexible heliac TJ-II [13] which, as we discuss below, shows similarities with other transitions described in the literature. In this work the formation of the shear layer is described from first principles in the framework of neoclassical theory and the turbulent phenomena that arise in the neighborhood of the transition are shown to be regulated by neoclassical transport. TJ-II [13] undergoes a spontaneous confinement transition typically at a line-averaged electron density $\bar{n}_e = n_{cr} \approx 0.6 \times 10^{19} \text{ m}^{-3}$. At this empirical critical density n_{cr} , the radial electric field E_r changes from positive to negative and, at the same time, a transport barrier is generated close to the edge. The reversal of E_r starts where the density gradient is maximum ($\rho \approx 0.8$, where $\rho = r/a$ is the normalized radius) and then prop-

agates across the entire region $0.5 < \rho < 0.9$ at a speed of the order of several m/s [14]. A sheared E_r always appears around the E_r -reversal point. Further increase in \bar{n}_e does not modify qualitatively E_r . It is argued [10] that the transport barrier is caused by turbulence reduction when the shearing rate of the $\mathbf{E} \times \mathbf{B}$ flow reaches values of the order of 10^5 s^{-1} ; that is, when it becomes comparable to the estimated linear growth rate of the resistive interchange instability in TJ-II [15].

Whereas similar transport barriers, related to jumps between roots of the ambipolar equation, have been observed in the low density regime of other stellarators [16], the very detailed study carried out in TJ-II has revealed additional interesting phenomena during the transition [9, 11]. First of all, the level of turbulence and the $E \times B$ flux are seen to increase prior to the transition, and this was later shown to be associated to long-range-correlated (LRCed) electrostatic potential structures that grow when approaching the critical density. These experimental results have historically led to an interpretation of the transition in terms of the paradigm of sheared flow generation by Reynolds stress and turbulence reduction by shear, see e.g. Refs. [8, 10]. Along the same line of reasoning, the peaking of the potential relaxation time in biasing turn-off experiments [10] and of the shear-flow susceptibility in electrode-biasing experiments [17] were interpreted in terms of an increased turbulent drive during the transition. The increase of the level of turbulence and of the long-range correlations are neither specific of this transition nor of stellarators: they are also observed in the L-H transition of TJ-II (which happens at higher \bar{n}_e) and of other devices, see e.g. Ref. [18] and references therein. We note that there are important differences between the low-density and the L-H transition (e.g. the improvement of energy confinement in the latter). Nevertheless, the neoclassical modelling of the L-H transition [19] also relies on bifurcations of the ambipolarity condition.

Since the inversion of E_r is an essential part of the transition, a neoclassical study of the transition is in order. The existence of multiple roots of the ambipolar

equation is a well-known feature of stellarators in the low-density regime [20]. Indeed, a static neoclassical calculation of E_r for plasmas immediately below (above) n_{cr} was performed in Ref. [21], yielding positive (negative) E_r in qualitative agreement with the experiment. In this work, we go beyond previous calculations and perform a full dynamical neoclassical calculation of the formation of the sheared E_r . We simulate the density ramp-up that leads to the transition and describe, from first principles, the formation and evolution of the shear flow in good agreement with the experiment. Furthermore, we show for the first time that the behaviour of the three quantities discussed above (amplitude of low-frequency LRCed potential fluctuations, potential relaxation time and shear-flow susceptibility) appear here as natural consequences of a neoclassical bifurcation. Namely, as the change of root approaches, the neoclassical poloidal viscosity (the restoring force of E_r deviations towards its ambipolar value), goes to zero. It will be shown that this automatically implies a maximum of the low-frequency plasma potential fluctuations, of the relaxation times and of the shear-flow susceptibility.

Let us begin by deriving the equation for the electric field evolution. We start from the momentum balance equation [5] summed over species:

$$m_i \frac{\partial(n\mathbf{u})}{\partial t} + \nabla \cdot \Pi_i + \nabla \cdot \Pi_e = \mathbf{j} \times \mathbf{B}. \quad (1)$$

Here, \mathbf{u} is the ion flow tangent to flux surfaces, Π_s is the viscosity tensor, $\Pi_s = m_s \int \mathbf{v}\mathbf{v}f_s(\mathbf{x}, \mathbf{v}, t)d^3\mathbf{v}$, or momentum flux of species s , f_s its distribution function, and $\mathbf{j} \times \mathbf{B}$ is the Lorentz force. Other forces (such as neutral friction) may be included as extra terms on the RHS of Eq. (1). We have assumed a quasineutral plasma consisting of singly charged ions and electrons ($n_e = n_i = n$). Note that we have dropped the inertia of the electrons, given their much lower mass m_s , but kept the electron viscosity tensor as it cannot be neglected in our low- n , high- T_e plasmas [22]. We work in Hamada magnetic coordinates (ψ, θ, ξ) , and follow the notation of Ref. [6]. The lowest order incompressible ion flow is conveniently written as:

$$\mathbf{u} = 2\pi \left(\frac{p'_i(\psi)}{n\epsilon} + \phi'(\psi) \right) \mathbf{e}_\theta + \Lambda(\psi)\mathbf{B}. \quad (2)$$

The flux surface label ψ is the toroidal magnetic flux and the prime stands for derivative. The first term on the RHS of Eq. (2) contains the diamagnetic and $E \times B$ perpendicular flows (p_i is the ion pressure, e the elementary charge, ϕ is the electrostatic potential, and $\mathbf{e}_\theta \times \mathbf{B} = (2\pi)^{-1}\nabla\psi$) together with the parallel Pfirsch-Schlüter flow ($\nabla \cdot \mathbf{e}_\theta = 0$ and $\langle \mathbf{e}_\theta \cdot \mathbf{B} \rangle = 0$ for a currentless stellarator). The term $\Lambda\mathbf{B}$ is the ion bootstrap flow [23]. If we project Eq. (1) along \mathbf{e}_θ and take flux-surface-average $\langle \cdot \rangle$ we obtain our evolution equation for

the radial electric field:

$$\begin{aligned} \frac{\partial E_r}{\partial t} = & \frac{1}{n} \frac{\partial}{\partial t} \left(\frac{p'_i(r)}{e} \right) - E_r \frac{1}{n} \frac{\partial n}{\partial t} + \\ & + \frac{(\psi'(r))^2}{4\pi^2 mn \langle \mathbf{e}_\theta \cdot \mathbf{e}_\theta \rangle} (e(\Gamma_e - \Gamma_i) + \langle \mathbf{j} \cdot \nabla r \rangle), \quad (3) \end{aligned}$$

where $E_r \equiv -\phi'(r)$ and the minor radius r is a geometric flux label defined in terms of the volume $V(r) \equiv \pi r^2 L_{\text{ax}}$, where L_{ax} is the length of the magnetic axis. We have obtained the radial particle fluxes from $\Gamma_s = -\frac{2\pi}{q_s \psi'(r)} \langle \mathbf{e}_\theta \cdot \nabla \cdot \Pi_s \rangle$ [24]. The viscosity tensor can be split into a neoclassical part, given by the gyrotropic pressure tensor, and an anomalous contribution:

$$\Pi_s = \Pi_s^{NC} + \Pi_s^{an} = p_{s\parallel} \mathbf{b}\mathbf{b} + p_{s\perp} (\mathbf{I} - \mathbf{b}\mathbf{b}) + \Pi_s^{an}. \quad (4)$$

As mentioned above, in non-quasisymmetric confining magnetic topologies [5], the leading order contribution to Eq. (3) is $\langle \mathbf{e}_\theta \cdot \nabla \cdot \Pi_s^{NC} \rangle$, being much larger than $\langle \mathbf{e}_\theta \cdot \nabla \cdot \Pi_s^{an} \rangle$, which will be therefore neglected. Higher order neoclassical terms like the shear-flow viscosity [5] can be considered. This term arises from orbit deviations away from flux surfaces and transforms Eq. (3) into a non-local diffusion equation for E_r . Since this complicates the discussion and does not fundamentally modify the predictions [26], we neglect it and provide a posteriori justification based on the experimental results.

We use the Drift Kinetic Equation Solver (DKES), complemented with momentum-correction techniques, to evaluate the pressure anisotropy in the TJ-II magnetic field in the parameter range usually found experimentally in the vicinity of the transition. Details of the calculation and convolution of the monoenergetic coefficients may be found in Ref. [23] and references therein. From Eq. (3), the time-evolution of E_r is fully determined if we know, at every instant of time, the magnetic configuration b_{mn} and the profiles n , T_e , T_i . Since we simulate a pure proton-electron plasma [22], the effective charge Z_{eff} (which mainly affects collisionality) is set equal to one. We perform a numerical simulation of a density ramp across the critical density for a plasma with profiles $n(\rho, t)$, $T_e(\rho, t)$ and $T_i(\rho, t)$ that mimic the experimental ones, see Fig. 1 and Refs. [9, 21]. We set $\langle \mathbf{j} \cdot \nabla r \rangle = 0$ unless otherwise stated. This is implied by quasineutrality ($\nabla \cdot \mathbf{j} = 0$), but a net radial plasma current can be induced in plasma biasing experiments. An important point to be noted is that, although we assume that the leading non-ambipolar particle fluxes are neoclassical, we make no particular assumption on the total particle or energy fluxes. They are included (together with the sources) implicitly in the evolution of n , T_e , T_i .

In Fig. 2 we sketch the evolution of the main quantities of our numerical ramp-up experiment in a representative radial position, $\rho = 0.7$. The evolution of E_r is given only by the evolution of n and T_e during the ramp-up. As n rises, the radial fluxes become larger and E_r less

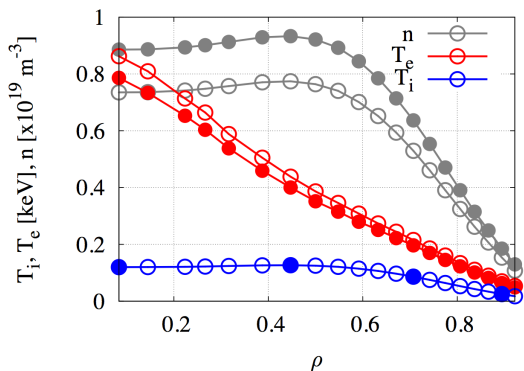


FIG. 1: (Color online) Plasma radial profiles for selected times: low (high) n in open (closed) circles. The evolution is given through $\frac{1}{n} \frac{\partial n}{\partial t} = 3 \text{ s}^{-1}$, $\frac{1}{T_e} \frac{\partial T_e}{\partial t} = -1.5 \text{ s}^{-1}$, and $\frac{\partial T_i}{\partial t} = 0$.

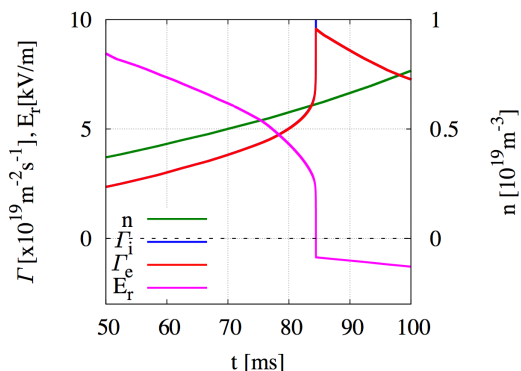


FIG. 2: (Color online) Time evolution of the relevant quantities at $\rho=0.7$ during the density ramp-up.

positive. Γ_i is slightly higher than Γ_e , which sets the sign of $\partial E_r / \partial t$, but the difference is not even visible in the figure. This is a consequence of the very slow variation of n and T_e , and will allow us to discuss some of the results in terms of the steady-state ambipolar equation. For $n \approx 0.6 \times 10^{19} \text{ m}^{-3}$, there is a change of root: E_r goes from positive to negative in several tens of μs . For larger n , further increase in n leads to smaller Γ_s and more negative E_r . This change of behaviour of Γ_s (they grow with n below n_{cr} and decrease above n_{cr}) might indicate a neoclassical particle transport barrier (nevertheless, let us remember that it is probably the ambipolar anomalous flux [9] which controls particle transport).

This general behaviour is expected for neoclassical simulations of TJ-II low-density plasmas [21, 22]. In Fig. 3, we show the ambipolar equation at $\rho = 0.7$ for several relevant times. Since we start from low collisionality, E_r is positive ($t = 10 \text{ ms}$). As n is raised, a negative stable root appears ($t = 50 \text{ ms}$ and $t = 80 \text{ ms}$), but the two stable

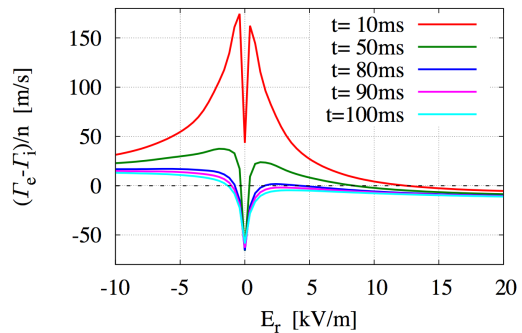


FIG. 3: (Color online) Ambipolar equation at $\rho=0.7$ for several representative times.

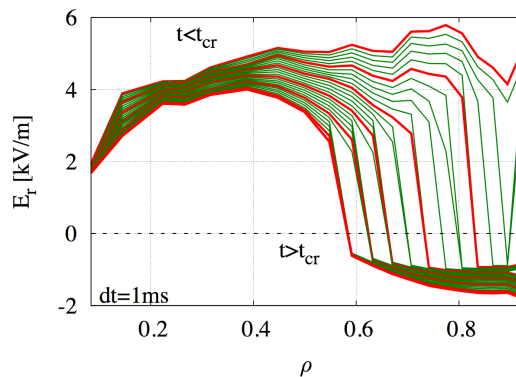


FIG. 4: (Color online) Radial electric field profile for representative times. Lines are separated by 1 ms and thick lines by 5 ms. The starting ($t < t_{cr}$) $E_r(\rho)$ is positive.

roots are separated by an unstable root, so E_r stays positive. Only for $n = n_{cr}$, when the electron root disappears ($t = 90 \text{ ms}$ and $t = 100 \text{ ms}$), the system *jumps* to negative E_r in tens of μs (the typical time of evolution towards ambipolarity, see below). Fig. 4 shows, for the first time, the formation and precise evolution of the shear layer in TJ-II plasmas. It starts to develop at $\rho = 0.85$, approximately where the gradient is maximum [9] and then propagates inwards and outwards: a speed of the order of 1 m/s may be extracted, as measured in Ref. [14]. Let us recall that, since we neglect the shear-flow viscosity, our simulations are local, hence the evolution equation for E_r is solved independently at each radial position, and only an indirect coupling exists through the n and T_e gradients. Thus, the speed of the layer propagation is determined basically by the evolution time of the local collisionality (as we have discussed, n and T_e). Shearing rates of the order of 10^5 s^{-1} can be inferred from Fig. 4, so this neoclassical shear might be large enough for playing a role in the reduction of turbulent transport (the linear growth rate of the resistive interchange instability,

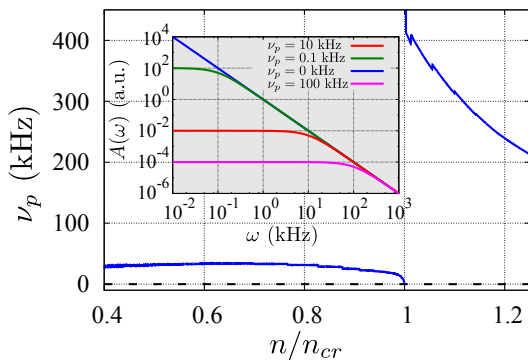


FIG. 5: (Color online) Density dependence of the neoclassical poloidal viscosity during the transition. n_{cr} is locally defined as the n at which E_r passes through 0 (inset: frequency dependence of the neoclassical damping for several values of μ_p).

that is thought to be the dominant one at the edge of TJ-II, is also of the order of 10^5 s^{-1} [15].

The main features of the low density transition are well captured by neoclassical transport and the correct prediction of the shear layer supports the initial ordering assumption. If the shear-flow viscosity had been calculated, the shear of E_r would be somewhat smaller [26], but this agreement with the experiment shows that no qualitative differences would have been found.

Generally, this picture is only slightly modified by considering the measured turbulent momentum transport. Indeed, local measurements of Reynolds stress [6] show average events $\Gamma_{RS}/n \lesssim 0.1 \text{ m/s}$ (which would not be perceptible in the evolution of E_r , see Fig. 3) and infrequent extreme events of $\Gamma_{RS}/n \lesssim 10 \text{ m/s}$ (which would not fundamentally modify the results). This is however not true when the transition is approached from below as can be seen in Fig. 3. In this situation ($t = 80 \text{ ms}$), the non ambipolar neoclassical fluxes display a weak dependence on E_r around the ambipolar value and large E_r excursions may be caused by turbulent momentum fluxes or external forcing (biasing) as is observed experimentally.

To make the argument more precise we define a neoclassical poloidal viscosity as the linear coefficient of the difference between the electron and ion radial fluxes (shown in Fig. 3) expanded around the ambipolar electric field, $[\Gamma_e - \Gamma_i](E_r) = -\mu_p(E_r - E_r^0) + O((E_r - E_r^0)^2)$. Eq. (3) then yields:

$$\begin{aligned} \frac{\partial E_r}{\partial t} &\approx \frac{e(\psi')^2}{4\pi^2 mn \langle \mathbf{e}_\theta \cdot \mathbf{e}_\theta \rangle} \left[\mu_p(E_r - E_r^0) - \frac{\langle \mathbf{j} \cdot \nabla r \rangle}{e} \right] \\ &= -\nu_p(E_r - E_r^0) + \check{j}_r. \end{aligned} \quad (5)$$

For the sake of argument we have neglected the (assumed slow) variations in n and T_i . The coefficient μ_p can be calculated directly from the data of Fig. 2, and we have

absorbed n , m , e , ψ' , $\langle \mathbf{e}_\theta \cdot \mathbf{e}_\theta \rangle$, and constants into ν_p and \check{j}_r . This scalar viscosity is a combination of the elements in the viscosity matrix defined in Ref. [25] (in particular, in the limit where the parallel currents are low and the temperature gradients small, it is proportional to the L_1 coefficient). The dependence of ν_p on n during the transition is shown in Fig. 5: it is smaller before the transition than after it (as predicted, with a simplified formulation, in Ref. [7]) and, more importantly, goes to zero when approaching n_{cr} from $n < n_{cr}$. We now show that the behaviour of the neoclassical viscosity provides a simple, unified explanation of the observed phenomena (amplitude of low-frequency, LRCed potential fluctuations, potential relaxation time and shear-flow susceptibility) that accompany the transition. To our knowledge, this is the first time that the vanishing of the neoclassical viscosity is explicitly shown to be enough to cause the phenomena at the transition.

The characteristic relaxation time in biasing turn-off experiments (ν_p^{-1} in Eq. 5) shows a peak around the critical density and decreases for larger density plasmas in the ion root [10]. This is reproduced by the curve shown in Fig. 5. Similarly, when a low frequency external biasing is applied, the response electric field is in phase with the biasing and its amplitude increases close to the critical density [17]. This is to be expected from Eq. 5, for in that case $E_r(t) \approx E_r^0 + \nu_p^{-1} \check{j}_r(t)$. Finally, to better discuss the observations of LRCs close to the transition [8] we Fourier transform Eq. (5):

$$\begin{aligned} i\omega \hat{E}_r(\omega) &= -\nu_p \hat{E}_r(\omega) + \hat{j}(\omega) \Rightarrow \\ |\hat{E}_r(\omega)|^2 &= \frac{1}{\nu_p^2 + \omega^2} |\hat{j}(\omega)|^2 \equiv A(\omega) |\hat{j}(\omega)|^2, \end{aligned} \quad (6)$$

for time scales faster than that of the density ramp, i.e., $\omega > \partial_t \log(E_r^0) \sim \partial_t \log(n) \sim 10 \text{ Hz}$. Eq. 6 shows that the amplitude of the fluctuations $\hat{E}_r(\omega)$ driven by a given broadband turbulent forcing $\hat{j}(\omega)$ is modulated by the neoclassical viscosity, which damps fluctuations of frequencies lower than ν_p . Below and above the transition (Fig. 5 inset), the fluctuations $\hat{E}_r(\omega)$ with $\omega \lesssim 10 \text{ kHz}$ are neoclassically damped. It is only close below n_{cr} that the neoclassical viscosity drops, leaving the low frequency E_r fluctuations (which are expected to display higher LRC) undamped. A higher order shear-flow viscosity [26] is usually included in Eq. (3), whose main effect is to smooth the radial variations of the E_r . For the present discussion, this term might only be important in the inner side of the shear layer, where the leading order viscosity goes to zero, and will set a low (though not null) effective viscosity and damping rate. The experimental measurement [10] of a peaking factor of about 5 in ν_p^{-1} gives an upper limit to these second order effects.

Note that the vanishing of the viscosity is a consequence of the transition from electron to ion root and the above phenomena are not to be expected in the reverse transition [12, 16].

In conclusion, we have described, by solving the drift kinetic equation, the formation of the shear layer in TJ-II. Even though such a first-principles theoretical calculation is by itself an important result, we have additionally advanced in the understanding of relevant physical phenomena associated to the transition, and also observed in other devices. They are essentially related to the amplification of dynamical electric fields as a result of the reduction or vanishing of the neoclassical viscosity.

Discussions with C. Hidalgo and the collaboration of the TJ-II team are acknowledged. This research was supported in part by grant ENE2009-07247, Ministerio de Ciencia e Innovación (Spain).

* joseluis.velasco@ciemat.es;
<http://fusionsites.ciemat.es/jlvelasco>

- [1] K H Burrell, *Phys. Plasmas* **4**, 1499 (1997).
- [2] F Wagner, *Plasma Phys. Control. Fusion* **49**, B1 (2007).
- [3] P. W. Terry, *Rev. Mod. Phys.* **72**, 109, 2000.
- [4] H. Sugama and T. Watanabe *Phys. Rev. Lett.* **94**, 115001 (2005).
- [5] P. Helander and A. N. Simakov, *Phys. Rev. Lett.* **101**, 145003 (2008).
- [6] J. A. Alonso, J. L. Velasco, J. Arévalo *et al.*, *Plasma Phys. Control. Fusion*, submitted (2012).
- [7] K. Itoh *et al.*, *Phys. Plasmas* **14**, 020702 (2007).
- [8] C. Hidalgo *et al.*, *Phys. Rev. E* **70**, 067402 (2004).
- [9] M. A. Pedrosa, C. Hidalgo, E. Calderón *et al.*, *Plasma Phys. Control. Fusion* **47**, 777 (2005).
- [10] M. A. Pedrosa, B. A. Carreras, C. Hidalgo *et al.*, *Plasma Phys. Control. Fusion* **49**, B303 (2007).
- [11] M. A. Pedrosa, C. Silva, C. Hidalgo *et al.*, *Phys. Rev. Lett.* **100**, 215003 (2008).
- [12] B. Ph. van Milligen *et al.*, *Nucl. Fusion* **51**, 113002 (2011).
- [13] C. Alejaldre, J. Alonso, L. Almuogueria *et al.*, *Plasma Phys. Control. Fusion* **41**, A539 (1999).
- [14] T Happel *et al.*, *Europhys. Lett.* **84**, 65001 (2008).
- [15] B. A. Carreras *et al.*, *Phys. Fluids B* **5**, 1491 (1993).
- [16] K. Ida, *Journal of Physics* **123**, 012004 (2008).
- [17] D. Carralero *et al.*, *Plasma Phys. Control. Fusion* **54**, 065006 (2012).
- [18] Y. Xu *et al.*, *Nucl. Fusion* **51**, 063020 (2011).
- [19] K. C. Shaing, *Phys. Rev. Lett.* **76**, 4364 (1996).
- [20] K. C. Shaing, *Phys. Fluids* **27**, 1567 (1984).
- [21] B. Zurro *et al.*, *Fusion Sci. Technol.* **50**, 419 (2006).
- [22] J. L. Velasco and F. Castejón, *Plasma Phys. Control. Fusion* **54**, 015005 (2011).
- [23] J. L. Velasco, K. Allmaier, A. López Fraguas *et al.*, *Plasma Phys. Control. Fusion* **53**, 115014 (2011).
- [24] S.P. Hirshman and D.J. Sigmar, *Nucl. Fusion* **21**, 1079 (1981).
- [25] H. Sugama and S. Nishimura, *Phys. Plasmas* **9**, 4637 (2002).
- [26] Y. Turkin *et al.*, *Phys. Plasmas*. **18**, 022505 (2011).